

Prediction of micro-channel flows using direct simulation Monte Carlo

H. Xue*, Q. Fan, C. Shu

Department of Mechanical and Production Engineering, National University of Singapore, 10 Kent Ridge Crescent, Singapore 119260, Singapore

Received 8 July 1998; received in revised form 10 April 1999; accepted 4 May 1999

Abstract

The direct simulation Monte Carlo (DSMC) method is a particle-based numerical modeling technique. It is recently used for simulating gaseous flow in micro-electro-mechanical-systems (MEMS) where micron-scale features become important. In this paper, numerical simulations of fluid flow in micro-channels are carried out using the DSMC method. The details in determining the parameters critical for DSMC applications in micro-channels are provided. Streamwise velocity distributions in the slip-flow regime are compared with the analytical solution based on the Navier–Stokes equations with slip velocity boundary condition. Satisfactory agreements have been achieved. Effects of the entrance and exit regions on simulation results are discussed. Simulations are then extended to transition flow regime ($Kn > 0.1$) and compared with the analytical solution. It is shown that the results are distinguished with the analytical solutions, which fail to predict the flow due to the break down of continuum assumption. It is indicated that the gradient of the pressure along the channel direction dominates the motion of the fluid flow. © 2000 Elsevier Science Ltd. All rights reserved.

Keywords: Direct simulation Monte Carlo; Micro-channel flows; Slip-flow regime; Transition flow regime

1. Introduction

Researches on Micro-Electro-Mechanical-Systems (MEMS) has become more prevalent, both in scientific inquiry and commercial applications [1]. The characteristic length scales that govern the momentum and energy transport between MEMS and their environments are typically of the order of microns. With the increasing demand of micron size mechanical devices, it is of great importance to understand the behavior of micro-fluid flows.

Numerical simulations can predict the fluid flow and heat transfer in mechanical devices and evaluate the performance of a new micro-device before hardware fabrication. The majority of computational fluid dynamics (CFD) methods for studying fluid flow are based on the Euler or the Navier–Stokes equations. MEMS, however, are often operated in gaseous environments at atmospheric conditions, where the molecular mean free path is approximately 70 nm. The ratio of the mean free path (λ) to the characteristic dimension (L) can be appreciable. This ratio, known as Knudsen number ($Kn = \lambda/L$), is used to indicate the degree of flow rarefaction. As it increases, the exchange of momentum and energy between the systems and the environment exhibits the behavior, which can be attributed to the discrete molecular composition of the environment. Generally, when $Kn >$

0.01, the rarefaction effect tends to be significant. Therefore, the traditional continuum based CFD becomes inaccurate when it simulates the flow around the devices with micron-size features because of the breakdown of the continuum assumption.

The direct simulation Monte Carlo (DSMC) method is a particle-based numerical modeling technique pioneered by Bird [2]. It computes the trajectories of a large number of particles and calculates macroscopic quantities by sampling particle properties. The principal steps of the DSMC are as follows: at the beginning of the simulation, the computational domain is divided into a net of cells, each particle is positioned inside the cell with a velocity and an internal energy. This is similar to the molecular dynamics method. The computation now proceeds in small discrete time step Δt , over which the motion of the particles and their interactions are uncoupled. Within one time step, all particles are first advanced according to their individual velocity. Then in each cell, a certain number of statistical collisions are computed by no-time-counter (NTC) method.

On the one hand, because the DSMC avoids the breakdown of continuum assumption in traditional CFD, it extends the validated range of numerical simulation. On the other hand, it has the advantage of being more efficient than other particles based methods because the place and time of a collision are no longer determined by computing the trajectories of all particles, but by means of a statistical consideration. Therefore, the DSMC becomes an attractive

* Corresponding author. Tel.: + 65-874-6479; fax: + 65-779-1459.
E-mail address: mpexueh@nus.edu.sg (H. Xue).

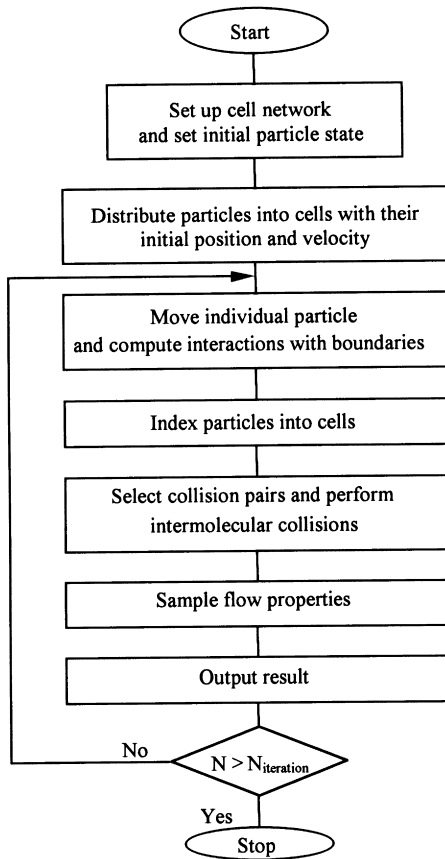


Fig. 1. DSMC flowchart.

tool to investigate the behavior of gaseous flows in micro-devices.

This paper presents numerical simulation on the gaseous micro-channel flow using the DSMC. Techniques on determination of parameters critical in the DSMC computation are provided. Simulation results are compared with available analytical solution. Effects of inlet and outlet of micro-channel on the flow behavior are discussed. Simulations are also extended to transition flow regime where Knudsen numbers are in the range of $0.1 < \text{Kn} < 3$.

2. Numerical modeling

2.1. Direct simulation Monte Carlo method

The DSMC method has been developed since 1970s as a powerful tool and efficient technique for computing rarefied gas flow [2,3,4]. DSMC models the flow as it physically exists: a collection of discrete particles each with a position, a velocity and internal energy. The states of particles are stored and modified with time as the particles move, collide, and undergo boundary interactions in simulated physical space. In a real gas, molecules move along their current trajectories until they strike another molecule or a boundary. But if the procedure is reproduced in numerical simulation,

such as molecular dynamics (MD), the computation quickly becomes unmanageable due to the increase of particles. One of defining assumptions in the DSMC is in response to this problem: a time step is chosen so that the movement and collision processes are uncoupled over the duration of it. The flowchart for a typical DSMC simulation is given in Fig. 1. A computational cell network representing physical space is first set up for the requirement of the selection of collision and the sampling of flow properties. The initial states of the gas such as vacuum and uniform equilibrium flow are prescribed. After the position and velocity of each particle is set, the method proceeds the iteration: (1) given a time step Δt , particles along their trajectories are displaced and interactions with boundary are calculated as they occur; (2) particles are sorted and their cell locations are rearranged; (3) collision pairs are selected and intermolecular collisions are performed on a probabilistic basis; (4) flow properties such as velocity, temperature, are obtained by sampling the microscopic state of particles in each cell.

The computational approximations associated with DSMC method are the ratio of the number of simulated molecules to the number of real molecules, the time step over which the molecular motion and collisions are uncoupled, and the finite cell and sub-cell sizes in physical space. The fundamental requirements are that the linear dimensions of the cells should be small in comparison with the scale length of the macroscopic flow gradients in the streamwise direction, which generally means that the cell dimensions should be of the order of the local mean free path, and the time step should be much less than the local mean collision time. Theoretically, the DSMC becomes more exact when the cell size and the time step tend to zero.

2.2. Mean free path

The conventional method to define the mean free path [3] is through recourse using the unrealistic hard sphere model which has a fixed diameter d and cross section $\sigma = \pi d^2$. The mean free path in an equilibrium gas of number density n is then

$$\lambda = (\sqrt{2}n\sigma)^{-1}. \quad (1)$$

The Chapman–Enskog result for the coefficient of viscosity in a hard sphere gas at temperature T is

$$\mu = \frac{5m}{16} \frac{(\pi RT)^{1/2}}{\sigma}, \quad (2)$$

where m is the molecular mass and R is the gas constant. The cross section may be eliminated from Eqs. (1) and (2) to give the standard result

$$\lambda = \frac{16\mu}{5} \frac{(2\pi RT)^{-1/2}}{\rho}, \quad (3)$$

where $\rho = nm$ is the gas density.

The inconsistency in the above procedure is that the

coefficient of viscosity has a fixed temperature exponent of 1/2, while the real gas coefficient of viscosity yields

$$\mu \propto T^\omega \quad (4)$$

where ω is generally in the range 0.6–0.9. Therefore, as an alternative scheme, a consistent definition of the mean free path, obtained through the variable cross-section hard sphere (VHS), was introduced by Bird [2]. The mean free path in a VHS is

$$\lambda = \frac{2\mu}{15} \frac{(7 - 2\omega)(5 - 2\omega)(2\pi RT)^{-1/2}}{\rho} \quad (5)$$

which can account for the real gas temperature exponent of the coefficient of viscosity, and is used in the present simulation.

2.3. Collision frequency

The mean free path is defined in a frame of reference moving with the stream speed of the gas and is therefore equal to the mean thermal speed \bar{c} of the molecular divided by the collision frequency, ν , i.e.

$$\lambda = \bar{c}/\nu. \quad (6)$$

The mean thermal speed \bar{c} in an equilibrium gas at temperature T is given by

$$\bar{c} = \frac{2}{(\pi^{1/2}\beta)} \quad (7)$$

where $\beta = (2RT)^{-1/2}$ is the reciprocal of the most probable molecular speed.

The combination of Eqs. (6) and (7) gives an expression of the collision frequency at temperature T , i.e.

$$\nu = \frac{2}{\lambda} \sqrt{\frac{2RT}{\pi}}. \quad (8)$$

2.4. Probabilistic nature of collision between molecule pairs

As one of the fundamental requirements, the computational time step (Δt) can be roughly estimated by $\Delta t \ll (1/\nu)$, i.e. the time step should be much smaller than the mean collision time.

The NTC proposed by Bird [2] for the DSMC is a generalized scheme, in which the number of collision pairs (N_p) considered in a given cell is computed through the equation,

$$N_p \propto \Delta t \frac{N_c^2}{n_{\text{ref}} V_c} \quad (9)$$

where V_c is the volume of a cell, N_c is the number of computational particles in the cell, n_{ref} is the simulated number density (the total simulated particles divided by the total simulated volume). NTC can overcome the defects of other generalized schemes [5], such as the time-counter scheme (TC) by Bird [2] and the null-collision scheme

(NC) by Koura [6]. The sensitive tests of the schemes for the evaluation of the lower limit of the mean molecular number per cell ($N_{c,\text{min}}$) were carried out by Koura [7] and Kaburaki et al. [8]. The recommended $N_{c,\text{min}}$ is between 4 to 30. Considering a DSMC cell of volume V_c in which each simulated molecule represents F_n real molecules, the probability P of collision between two simulated molecules over the time interval Δt is proportional to the product of their relative speed c_r and total cross-section σ_T , i.e.

$$P = F_N \sigma_T c_r \Delta t / V_c \quad (10)$$

The average number of real molecules in the cell is nV_c and averaged number of simulated molecules is $N = nV_c/F_N$. The full set of collisions can be calculated by selecting, in turn, all $N(N-1)/2$ pairs in the cell and by computing the collisions with probability P . In order to carry out the simulation more efficient, only a fraction of the pairs are chosen. The resultant probability is increased by dividing Eq. (10) by this fraction. Hence,

$$P_{\text{max}} = F_N (\sigma_T c_r)_{\text{max}} \Delta t / V_c \quad (11)$$

In the NTC method, $(1/2)N\bar{N}F_N(\sigma_T c_r)_{\text{max}} \Delta t / V_c$ pairs are chosen from the cell at the time step, where N is a fluctuating quantity and \bar{N} is an average value. The collision is then computed with probability $\sigma_T c_r / (\sigma_T c_r)_{\text{max}}$.

2.5. Total simulated particles and computational time

Based on above discussion, the total number of the simulated particles (N_{tot}) is equal to the product of the average number of simulated molecules per cell and the total number of cells in flow field (C_{tot}), i.e.

$$N_{\text{tot}} = N_c C_{\text{tot}} \quad (12)$$

One of the aforementioned requirements is that the cell dimension is of the order of the local mean free path. According to above expression, N_{tot} is restricted by the capability of computational resource. As the linear dimension of the micro-channels increases, it becomes computationally impractical to maintain the two requirements: the cell size should be of the order of the mean free path and there should be enough particles in the cell. This means the possible scale of a micro-channel in which the simulations can be carried out is limited by the capability of the current workstations or supercomputers. For example, one of our computations simulates a physical space of $30 \times 1.12 \mu\text{m}^2$, which is divided into 300×20 sampling cells, and each cell consists of 2 collision subcells. The total number of simulated particles is about 2.4×10^5 . Nearly 20 particles are located in one collision subcell. The total number of samplings is 1.3×10^4 . When the calculation was performed on the Cray J916 supercomputer, the approximate CPU time and memories consumed were 7.12 h and 100 MB respectively.

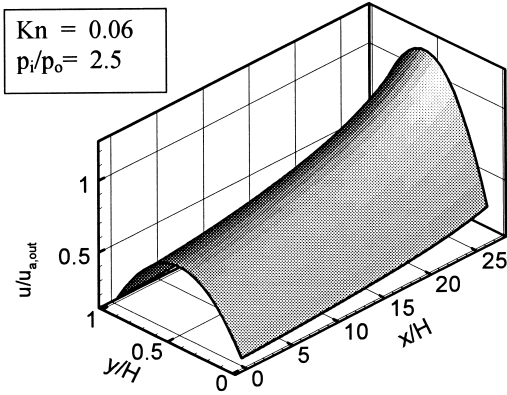


Fig. 2. Analytical streamwise velocity distribution ($Kn = 0.06$).

2.6. Boundary conditions

Modeling the interaction of gas molecules with solid surface plays an important role in the DSMC simulation. But there is no model of gas-surface interaction that is adequate over a wide range of factors for all combinations of gases and surfaces. Some analytical and numerical simulations are based on the assumption of diffuse reflections with full thermal and momentum accommodation [9]. Recently, the Cercignani_Lampis_Lord (CLL) gas-surface model [10] has been generally accepted in the DSMC simulations, which is also used in the present simulation.

At inlet and outlet boundaries, the physical states of particles should be determined to avoid poorly formulated inflow and outflow treatment [11,12]. To reproduce the pressure-driven flow, the pressures at inlet and outlet are prescribed. The most probable molecular thermal velocity of the introduced molecules is determined in accordance with the temperature given at inlet. The thermal velocity components perpendicular to the inlet and outlet boundaries are assigned to the incoming particles. Other variables at both inlet and outlet have to be specified from the states of particles inside the flow field. For example, at inlet, it is critical to determine the streamwise velocities of the incoming particles from the states of the particles inside the computational region. Our

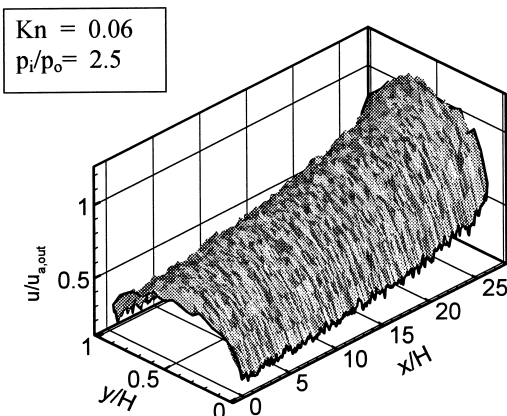


Fig. 3. Computed streamwise velocity distribution ($Kn = 0.06$).

method is to initialize them as zero at the beginning and specify them every iteration according to the average streamwise velocities of the particles in the cells along the inlet.

3. Results and discussions

3.1. Analytical and simulated results in slip flow regime

The investigation of Harley et al. [13] demonstrated the existence of nonzero wall velocity in micro-channels and showed the contribution of the nonzero slip velocity on the pressure drop. According to Arkilic et al. [14], the two-dimensional time-invariant Navier–Stokes equations can be solved analytically for a compressible fluid in the slip flow regime when the common boundary condition of non-slip wall is replaced by a Kn -dependent slip-wall velocity condition, given by

$$u_{\text{wall}} = \frac{2 - F}{F} Kn \frac{du}{dy} \Big|_{\text{wall}} \tag{13}$$

where u is the streamwise velocity, Kn is the local Knudsen number, y is the transverse coordinate which is zero at the centerline of the channel, F is the tangential momentum accommodation coefficient which is assumed to vary between zero (specular reflection) and unit (diffuse reflection). The pressure distribution along the length of the micro-channel is expressed as a function of location in the micro-channel direction and overall pressure ratio is

$$P_x = -6\sigma Kn_o + \sqrt{(6\sigma Kn_o)^2 + (P_i^2 + 12\sigma Kn_o P_i) \left(1 - \frac{x}{L}\right) + (1 + 12\sigma Kn_o) \frac{x}{L}} \tag{14}$$

where $P_x = p(x)/p_0$ is the ratio of the local pressure and the outlet pressure, $\sigma = (2 - F)/F$ represents the streamwise momentum accommodation, Kn_o is the outlet Knudsen number, x is the coordination in the channel direction, and L is the channel length. Meanwhile a theoretical streamwise velocity distribution can be written as

$$u(x) = \frac{1}{2\mu} \frac{dp}{dx} \left(y^2 - \frac{H^2}{4} - \sigma H^2 Kn \right) \tag{15}$$

where μ is the coefficient of viscosity, and H is the channel height.

After velocities are normalized by the area-averaged streamwise velocity $u_{a,\text{out}}$ at the channel exit, Eq. (15) is plotted in Fig. 2. It is seen that important features of conventional hydrodynamic flow no longer exist. For instance, transverse velocity component v and the gradient of the streamwise velocity component $\partial u/\partial x$ are not everywhere zero. Instead, several unique features are observed. For maintaining a constant mass flow, the mean streamwise velocity increases to make up the density drop caused by

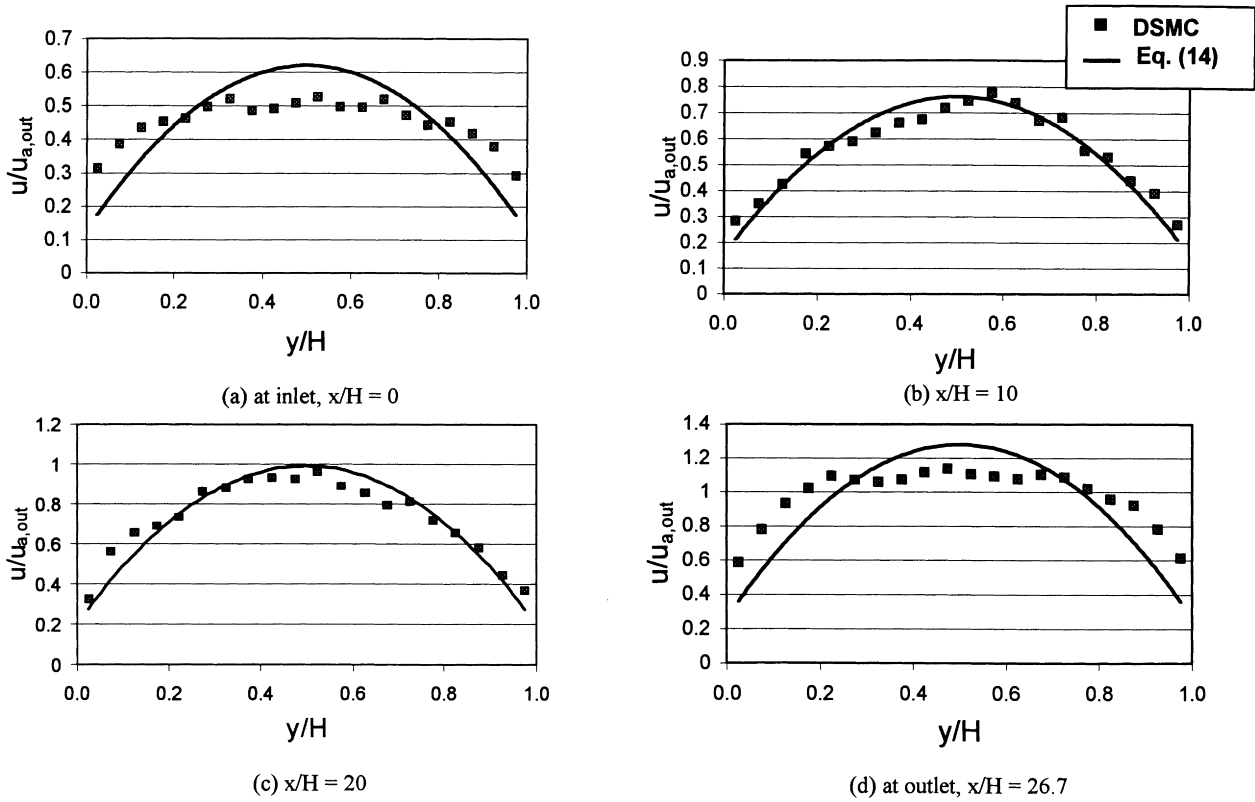


Fig. 4. Comparisons of predicted and analytical velocity distributions at different cross sections of the micro-channel.

the decrease of the pressure in the channel direction. The velocities at walls are nonzero and increase in the stream-wise direction.

The DSMC result is presented in Fig. 3. Compared with the analytical velocity profile shown in Fig. 2, the simulation successfully reproduced the mean flow acceleration due to compressibility and the slip flow effect demonstrated by the theory due to rarefaction. The detailed comparisons are shown in Fig. 4. Remarkable agreements are achieved between the predicted and analytical results in Fig. 4(b) and (c), where the flow is considered to be fully developed. In fact, the agreement is observed along the channel from $x/H = 10$ up to $x/H = 25$. However, significant discrepancy is seen in the regions near the inlet and close to the outlet.

Examining the assumptions used in the analytical model [14], we were not surprised with above disagreement at the inlet and outlet. In analytical solution, boundary conditions are imposed so that the effects of inlet and exit are eliminated. However, in the DSMC, uniform velocity distribution is assumed at the inlet, and pressures at inlet and outlet are specified. The results of DSMC indicate that the inflow effects are not negligible at the entrance region, which persists up to almost $x/H = 10$. Compared with the entrance region, affected length in exit region is short. In fact, the DSMC provides a technique to study flow development and the velocity distribution at the hydrodynamic entrance region, in which there is no available analytical solution.

3.2. Simulated results in transition flow regime

Advantage can be taken of the fact that the DSMC method is valid in all Knudsen number regimes. DSMC is therefore an attractive tool for investigating the effects of rarefaction from slip flow regime ($0.01 < Kn < 0.1$) to transition flow regime ($0.1 < Kn < 3$). In transition regime, the mean free path is comparable to the characteristic dimension of the flow. The analytical solution of Navier–Stokes equations (even with the slip flow boundary condition) becomes inaccurate. On the other hand, the degree of

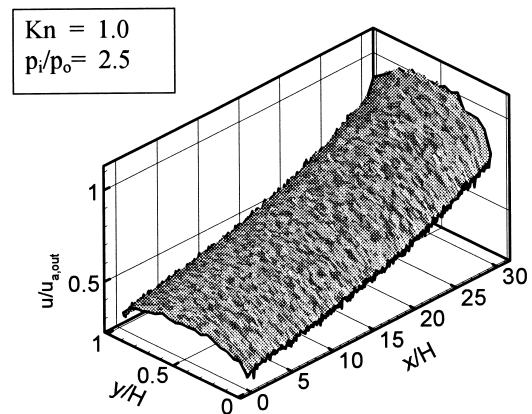


Fig. 5. Computed streamwise velocity distribution ($Kn = 1.0$).

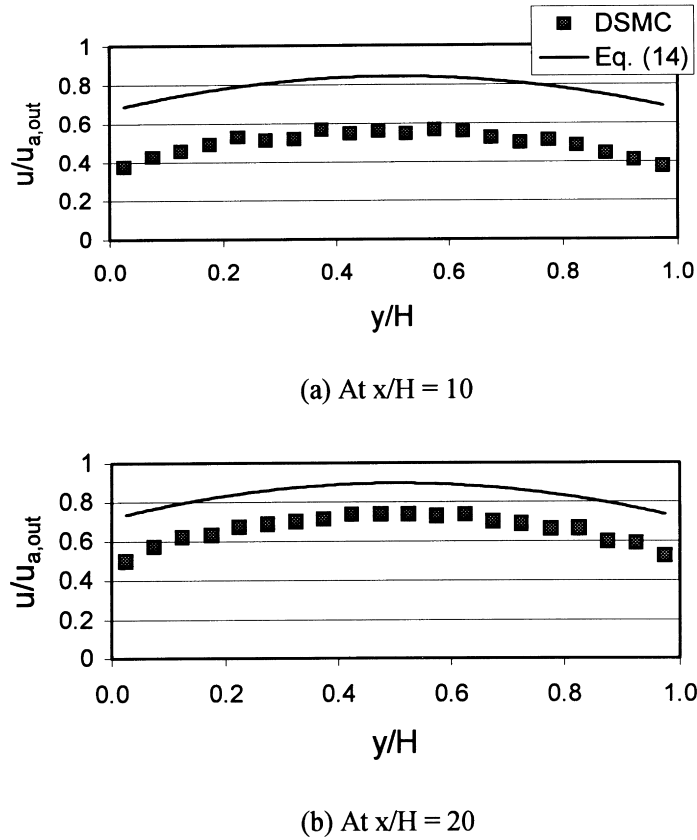


Fig. 6. Comparisons of computed and analytical velocity distributions at different cross sections of the micro-channel for $Kn = 1.0$.

rarefaction is not high enough to solve the collisionless Boltzmann equation directly.

Simulations are carried out under different Knudsen numbers that are specified as 0.174, 1, and 2.79 respectively.

One of the DSMC results for $Kn = 1$ and the pressure ratio $P(x) = 2.5$ is plotted in Fig. 5. To compare with the analytical prediction, the DSMC velocity distributions in the micro-channel at $x/H = 10$ and $x/H = 20$ are shown in Fig. 6. It is noted that the significant discrepancy between DSMC and analytical solution occurs even in fully developed

region. The results demonstrate the capability of the DSMC in simulating the micro-flow when $Kn > 0.1$.

The failure of the analytical solution is stemmed from the continuum assumption of the Navier–Stokes equations, which can be derived from the Boltzmann equation based on the Chapman–Enskog expansion of the velocity distribution function f , by approximating it to the first order of Knudsen number. Naturally, the Navier–Stokes equations break down in the transition regime ($Kn > 0.1$). They have to be substituted either by the Boltzmann equation or by

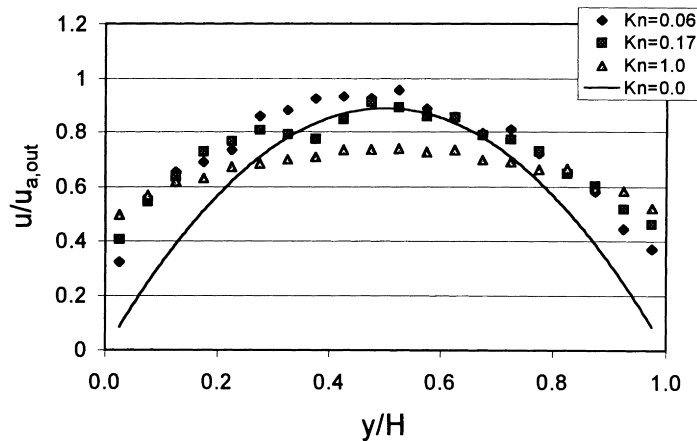


Fig. 7. Comparison of velocity profiles with different Knudsen numbers at $x/H = 20$.

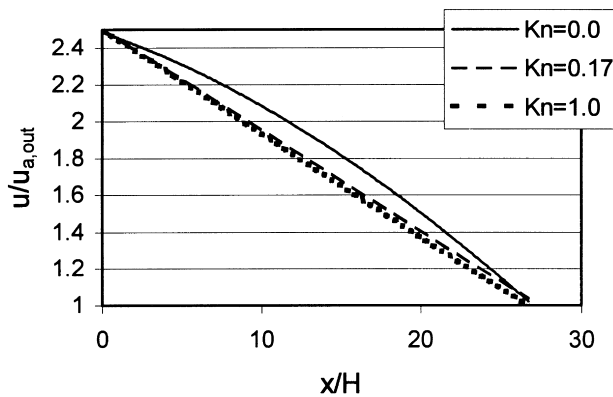


Fig. 8. Pressure distributions along the micro-channel at different Knudsen numbers.

continuum approximations that include higher order modifications of the stress tensor and heat flux terms (e.g. the Burnett equations). On the other hand, the DSMC is known as a particle method for the analysis of collisional flow. Nanbu [4] proved that the algorithms used in the DSMC are subsequently derived from the Boltzmann equation, rather than from physical arguments.

The dependence of the velocity distributions upon the increase of the Knudsen number is plotted in Fig. 7. It shows that the shapes of velocity distributions are getting flatter when the Knudsen number increases. The profile of the velocity at $Kn = 1$ has lost the parabolic feature which can be found at $Kn = 0.06$. Meanwhile, the local maximum velocity is reduced while slip velocity gets higher with the increase of the Knudsen number.

As expected, the non-linear pressure distribution along the direction of micro-channel is observed due to the compressibility of the flow. The simulated pressure distributions are compared with the analytical prediction in Fig. 8. With the reference of the continuum curve ($Kn = 0.0$), the non-linearity becomes less pronounced when the Knudsen number is increased. This finding is consistent with the result obtained by Piekos and Breuer [11]. Comparing the velocity distribution in slip flow regime (Fig. 3) to that in transition flow regime (Fig. 5), it is found that the shapes of streamwise velocity components in x direction becomes flatter as the Knudsen number increases. The linearity of pressure curve and streamwise velocity distribution in x direction increases coincidentally with enhanced rarefaction from slip flow to transition flow regime. This implies that the gradient of the pressure along the direction of micro-channels dominates the motion of the gas for the pressure-driven micro-flows.

4. Conclusion

The DSMC method is a powerful tool to investigate the behavior of flows in micro-channels in which continuum-based fundamental assumption might break down. Detailed

descriptions of the DSMC application in micro-channel has been presented.

The DSMC results for a slip flow regime micro-channel were compared with the analytical solution of Navier–Stokes equations developed by Arkilic et al. [14]. Excellent agreements have been achieved in fully developed flow region. By introducing appropriate inlet and outlet boundary conditions, the DSMC can account for the effects of hydrodynamic entrance and exit regions, and predict the flow behavior in these regions, which are neglected in the analytical solution.

The DSMC simulations are extended to the transition flow regime. The results are distinguished with the analytical solutions, which fail to predict the flow due to the break down of the continuum assumption. It is found that the compressibility of a pressure-driven flow is negated by the rarefaction in pressure-driven flow. The gradient of the pressure along the channel direction dominates the motion of the flow. This is indicated by the coincident change of linearity of the pressure curve and the streamwise velocity distribution in the direction of micro-channel.

References

- [1] Fan LS, Tai YC, Muller RS. Integrated movable micromechanical structures for sensor and actuators. *IEEE Transaction on Electronic Devices* 1988;35(6):724–30.
- [2] Bird GA. *Molecular gas dynamics and the direct simulation of gas flows*. New York: Oxford University Press, 1994.
- [3] Bird GA. Definition of mean free path for real gases. *Physics of Fluids* 1986;26(11):3222–3.
- [4] Nanbu K. Theoretical basis of the direct simulation of Monte Carlo method. In: Teubner BG, editor. *Proceedings of the 15th international symposium on rarefied gas dynamics*, Stuttgart, vol. 1, 1988. p. 369–83.
- [5] Abe T. Generalized scheme of the no-time-counter scheme for the DSMC in rarefied gas flow analysis. *Computers in Fluids* 1993;22(2/3):253–7.
- [6] Koura K. Null-collision technique in the direct-simulation Monte Carlo method. *Physics of Fluids* 1986;29(11):3509–11.
- [7] Koura K. A sensitive test for accuracy in evaluation of molecular collision number in the direct-simulation Monte Carlo method. *Physics of Fluids* 1990;A2(7):1287–9.
- [8] Kaburaki H, Yokokawa M. Computer simulation of two-dimensional continuum flows by the direct simulation Monte Carlo method. *Molecular Simulation* 1994;12(3-6):441–4.
- [9] Piekos ES, Breuer KS. DSMC modeling of microchanical devices, *AIAA Paper* 1995-2089.
- [10] Lord RG. Some extension to the Cercignani–Lampis gas-surface scattering Kernel. *Physics of Fluids* 1991;A3(4):706–10.
- [11] Piekos ES, Breuer KS. Numerical modeling of micromechanical devices using the direct simulation Monte Carlo method. *Journal of Fluids Engineering: ASME* 1996;118:464–9.
- [12] Anderson JD. *Modern compressible flow with historical perspective*. New York: McGrawHill, 1990.
- [13] Harley J, Huang Y, Bau H, Zemel J. Gas flow in micro-channels. *Journal of Fluid Mechanics* 1995;284:257–74.
- [14] Arkilic EB, Breuer KS, Schmidt MA. Gaseous flow in microchannels. *ASME FED* 1994;197:57–65.